Journal of Intelligent & Robotic Systems (2022) 105: 29
https://doi.org/10.1007/s10846-022-01644-x

SHORT PAPER

# Bionic Fish Trajectory Tracking Based on a CPG and Model Predictive Control

Zheping Yan[1] · Haoyu Yang[1] · Wei Zhang[1] · Qingshuo Gong[1] · Fantai Lin[1] · Yu Zhang[1]

Received: 13 October 2021 / Accepted: 23 April 2022 / Published online: 17 May 2022


## Abstract

Bionic fish have received widespread attention due to their high mobility, high concealment and high propulsion efficiency. Trajectory tracking and tracking accuracy are the main challenges in controlling the motion of bionic fish. To realize the trajectory tracking control of bionic fish, in this paper, nonlinear dynamics model of bionic fish is established by the Newton-Euler equation and Denavit-Hartenberg (D-H) coordinate transformation, and it is reasonably simplified. Then, a model predictive controller is established based on the dynamic model, and combined with a central pattern generator (CPG) network, a CPG-based model predictive controller (MPC-CPG controller) is proposed. Finally, simulations and experiments are carried out on the bionic fish, tracking the circular trajectory and straight trajectory. Experiments show that under the condition of initial error, the MPC-CPG controller can quickly eliminate the position error and heading angle error of the bionic fish, and track to the reference trajectory. For the tracking circular trajectory and straight trajectory, the position errors are kept at $-6.9\% \sim 14.9\%$ and $-8.6\% \sim 8.6\%$ of the body length, respectively, and the heading angle errors are always kept at $-4.76° \sim 4.73°$ and $-3.24° \sim 3.55°$, respectively. Experiments verify the effectiveness of the proposed MPC-CPG.

**Keywords** Bionic fish · Dynamics · CPG · Model predictive control · Trajectory tracking

## 1 Introduction

With the continuous deepening of human development in the ocean, the diversity and complexity of underwater operations have also increased, and the shortcomings of traditional autonomous underwater vehicles in terms of manoeuvrability, concealment and propulsion efficiency have become increasingly obvious. After long-term genetic evolution and natural selection, natural fish have evolved extremely well in terms of their underwater sports abilities. Inspired by this, scholars have imitated various fish and have developed bionic tuna [1], bionic pike fish [2], bionic dolphins [3], bionic whale sharks [4], etc. Compared with traditional underwater unmanned vehicles (UUVs), bionic fish have the advantages of low noise, good mobility, and harmlessness to underwater creatures [5], so they are widely used in complex underwater tasks [6, 7].

Although research on bionic fish has achieved remarkable results, there is still a large gap in sports performance compared with fish in nature [8]. At present, the methods commonly used to control the motion of bionic fish include the fish body wave curve fitting method based on a rod structure, the simple sinusoidal controller method and the motion control method based on a central pattern generator [9]. The fish body wave curve fitting method based on a rod structure has the advantage of simple modelling, but it has many shortcomings in terms of manoeuvrability and flexibility [10]. The sinusoidal controller method is simple to control and can generate diversified swimming gaits online, but it cannot achieve a smooth and natural transition when the frequency and amplitude change suddenly [11]. A central pattern generator is a type of neuronal circuit widely found in invertebrates and

✉ Wei Zhang
yanghaoyu1993@126.com

Zheping Yan
810347920@qq.com

Haoyu Yang
yanghaoyu@hrbeu.edu.cn

Qingshuo Gong
1966284685@qq.com

[1] College of Intelligent Systems Science and Engineering, Harbin Engineering University, No. 145, Nantong Street, Harbin 150001, Heilongjiang, China

vertebrates. It generates stable phase-locked periodic signals through mutual inhibition between neurons and controls the rhythmic movement of related parts of the body, such as breathing, walking, and flying. [12]. The CPG model contains highly nonlinear terms, which leads to many difficulties in theoretical research and applications, but it still has incomparable superiority compared with traditional motion control methods [13]. A central pattern generator has the advantages of good stability, strong robustness, smooth transition, and easy adjustment. Therefore, central pattern generators have received increasing attention and are widely used in the motion control of various robots. Knuesel Jeremie applied a CPG network to a bionic salamander and realized five movement modes and movement mode switching of the bionic salamander in an amphibious environment [14]. Chen JY et al. used central pattern generator-controlled bionic fish to achieve tasks such as avoiding static obstacles, avoiding moving obstacles, and tracking designated directions [15].

Although the introduction of a CPG to control robot motion improves the coordination and smoothness of the motion, because a CPG is open-loop, to achieve more intelligent motion, it is necessary to add feedback items or use upper-level algorithms for adjustments. Cao Y et al. developed a bionic fish that uses an improved phase oscillator as the basic unit of a central pattern generator network. On this basis, a central pattern generator fuzzy algorithm was developed to control the bionic fish to perform stable three-dimensional motion and complete bionic fish experiments on open-loop speed control, depth and yaw closed-loop control [16]. Wang Gang et al. proposed an adaptive gait control method based on a central pattern generator and feedforward neural network. On this basis, two reflection mechanisms were proposed to achieve adaptive gait control on complex terrain, and waveform gait generation and adaptive movement ability on uneven ground were verified through experiments [17]. Aiming at the motion characteristics of a snake-like robot, Bing ZS et al. proposed a control method based on a lightweight central pattern generator for sliding gait conversion that effectively solved the problem of instability and abnormal torque generated by the robotic snake when changing its speed, direction and body shape [18].

To improve the motion performance of bionic robots, some scholars have also been dedicated to optimizing the parameters of central pattern generator networks. For example, Yu Junzhi and Wang Ming et al. used a dynamic model and particle swarm optimization (PSO) algorithm to solve the optimal central pattern generator's parameters, thereby improving the swimming speed and propulsion efficiency of bionic fish [19, 20]. Wang Y et al. normalized the limit cycle of the Matsuoka central pattern generator and input the normalized central pattern generator signal and feedback information into the neural network for learning. Thus, a control signal that removed the shape information of the central pattern generator network and retained only the time information was generated. Experiments have shown that this method can effectively improve the adaptability of a robot to the environment [21].

To ensure that an underwater robot can efficiently and accurately complete various special underwater tasks, it is necessary to carry out further research on the space motion control technology of the robot [22]. Trajectory tracking is one of the key technologies for autonomous robots to perform tasks. It requires the actual state of the robot to meet the constraints of the reference trajectory in time and space. At present, the methods used for robot trajectory tracking control mainly include backstepping control, model predictive control, sliding mode control, neural networks, and robust adaptive control [23]. Yang et al. introduced a recurrent neural network (RNN) into the terminal sliding mode control method to effectively realize the high-precision trajectory tracking control of a robot under the influence of uncertain factors [24]. Sun et al. proposed a cascaded dynamic trajectory tracking control method based on model predictive control and sliding mode control and solved the problems of modelling uncertainty and external interference [25].

However, because bionic fish have a high degree of nonlinearity and under driving characteristics, trajectory tracking control is challenging. At present, there are few studies on the trajectory tracking control of bionic fish. Wang Ming et al. used an iterative learning method to control the trajectory tracking of bionic fish and conducted simulation verification [26]. Zheng XW et al. established a dynamic model of a bionic fish with a centre of gravity adjustment mechanism and a multimovement fin drive mechanism. Based on the dynamic model, trajectory tracking was carried out through model predictive control [27].

There are many constraints in the motion of bionic fish, and model predictive control can explicitly incorporate the multiconstraint problem into rolling optimization. At present, MPCs have been widely used in the motion control of various robots (unmanned aerial vehicles, unmanned ground vehicles, unmanned underwater vehicles, etc.) and has achieved good results [28]. Aiming at the trajectory tracking problem of bionic fish, this paper uses a MPC as the upper trajectory tracking controller and CPG as the bottom motion controller. The controller can not only consider the input constraints and state constraints of the system and improve the ability of an underwater robot to operate stably but also improve the coordination and smoothness of motion in the process of trajectory tracking.

The main intellectual contributions of this paper are as follows: First, we established a nonlinear dynamic model of a bionic fish through the Newton-Euler equation and the D-H coordinate transformation, and the dynamic model was reasonably simplified. Then, based on the dynamic model, a model predictive controller was established, and combined with the CPG network, a CPG-based model predictive

controller (MPC-CPG) was proposed. Finally, simulations and prototype experiments were performed to verify the effectiveness of the proposed MPC-CPG in the trajectory tracking process.

The rest of the paper is organized as follows: Section 2 introduces the system design and dynamic modeling of the bionic fish. Section 3 describes the problem formulation, and an MPC-CPG is established for bionic fish trajectory tracking. In Section 4, the effectiveness of the control method proposed in Section 3 is verified by simulations and experiments. Finally, Section 5 gives conclusions.

## 2 Bionic Fish Design and Modeling

### 2.1 Overview of the Bionic Fish

As shown in Fig. 1, according to the shape and movement characteristics of a shark, a bionic shark was developed as a controlled platform. Compared with the real shark, the bionic shark only retains the tail fin and a pair of pectoral fins as the motion actuators, which are driven by three servo motors. The dorsal fin is equipped with a wireless communication module fixed on the shell, and the other fins are ignored. The shell of the bionic fish is made of a carbon fibre composite material. The tail fin is fixed on a set of gear linkage mechanisms, and only one motor is needed to drive the three joints. The core controller consists of an NVIDIA development board equipped with an ROS system and an STM32 microcontroller unit, which collect signals from sensors such as depth sensors and an IMU. Table 1 lists the detailed technical parameters of the bionic fish.

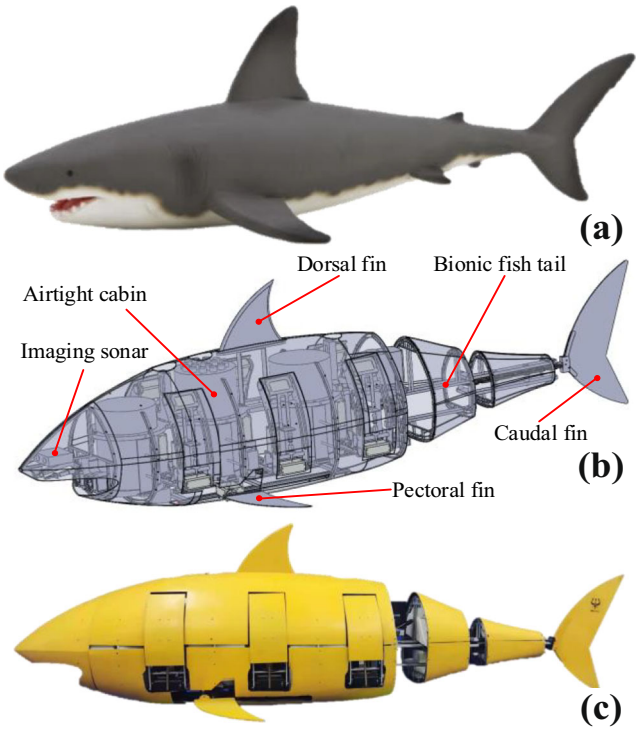


**Fig. 1** Model diagram and prototype of bionic fish

### 2.2 Nonlinear Dynamic Model of the Bionic Fish

Because the interaction between the bionic fish and a fluid when swimming is complex and highly nonlinear, especially at high Reynolds numbers [29], there is no mature and unified dynamic model. Current methods used to construct bionic fish dynamics models mainly include computational fluid dynamics (CFD) simulation evaluation [30] and a dynamic model constructed with the Lagrange equation or Newton–Euler equation combined with potential flow theory [2, 31, 32]. Compared with other modelling methods, the Newton–Euler equation has the advantages of being simpler and more intuitive, but also, the established dynamic model is easy to write in the form of CPG parameters, which is convenient for combining with an MPC. Therefore, in this paper, the Newton–Euler equation is used to model the dynamics of the bionic fish, and through D–H coordinate transformation, a dynamic model conforming to the caudal fin propulsion mechanism proposed in this paper is constructed. A schematic diagram of the bionic fish tail is shown in Fig. 2.

According to the gear transmission relationships, the relative rotation angle of each joint $\theta_i$ can be obtained as

$$\begin{aligned} \theta_2 &= i_1\theta_1 \\ \theta_3 &= i_2\theta_1 \end{aligned} \tag{1}$$

where $i_1 = z_1 \frac{z_3}{z_2} z_4{-}1$, $i_2 = \frac{z_5}{} z_8(z_1 \frac{z_3}{z_2} z_4{-}1)$, and $z_i$ is the number of teeth of gear $i$.

The hydrodynamic forces of the fish body and fish tail are equivalent to the concentrated forces acting on each particle $J_i$ of the fish. The coordinate systems and forces of the established bionic fish are shown in Fig. 3; among them, XOY and xoy are the geodetic coordinate system and the body coordinate system, respectively. $F_{fx}$ and $F_{fy}$ are the fluid resistances when the bionic fish swims, and $F_1 \sim F_5$ are the hydrodynamic forces when the bionic fish swims.

The nonlinear dynamic model of the bionic fish is established by the Newton-Euler equation as

**Table 1** Technical parameters of the bionic fish prototype

| Parameter | Description |
|---|---|
| Size ($m^3$) | 1.74×0.75×0.62 |
| Weight (kg) | 42.7 |
| Number of motors | 3 |
| Power supply (V) | DC 24 |

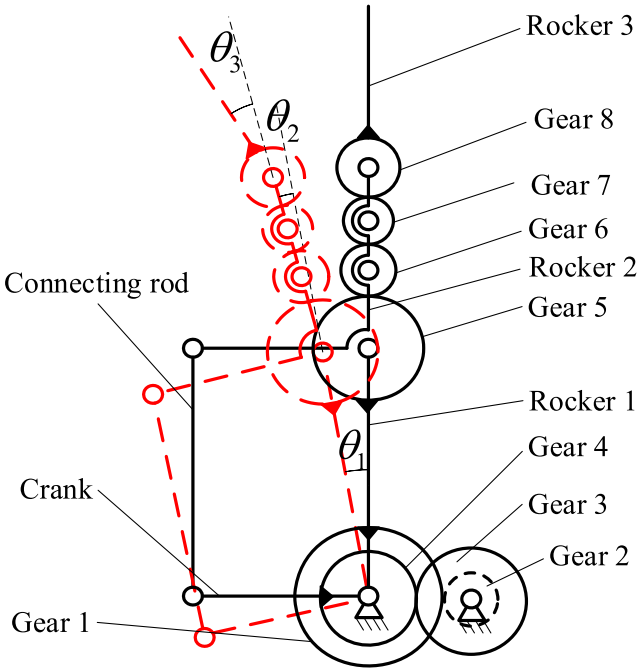


**Fig. 2** The schematic diagram of the caudal fin propulsion mechanism

$$\begin{aligned} m\ddot{x} &= -F_{1x} + F_{2x} + F_{3x} + F_{4x} + F_{5x} - F_{fx} \\ m\ddot{y} &= F_{1y} - F_{2y} + F_{3y} + F_{4y} + F_{5y} - F_{fy} \\ I_z\ddot{\varphi} &= -F_1 l_1 - F_2 l_2 + F_3 l_3 + F_4 l_4 + F_5 l_5 \\ \dot{X} &= \dot{x} \\ &= \dot{x}sin\varphi + \dot{y}cos\varphi \end{aligned} \quad cos\varphi - \dot{y}sin\varphi\dot{Y} \tag{2}$$

where X, Y and $x$, $y$ are the positions of the bionic fish in the geodetic coordinate system and the body coordinate system, respectively. $l_i$ is the force arm from the hydrodynamic force $F_i$ to the rotation centre $O_1$ of the bionic fish; $\varphi$ is the heading angle; and $I_z$ is the moment of inertia around the z-axis.

To simplify the calculation process, the resistance formula of a simple flat plate is used to calculate the hydrodynamic force.

$$F_i = C_i \rho v_{Ji}^2 S_i / 2 \tag{3}$$

where $C_i$ is the drag coefficient of each part of the fish body, $C_1 \sim C_5$, $C_x$, $C_y$; $v_{Ji}$ is the speed at the centre of mass of each part of the fish body and tail, $v_{J1} \sim v_{J5}$; $\dot{x}$ and $\dot{y}$ are the longitudinal speed and lateral speed of the bionic fish, respectively; $S_i$ is the area of slapping water of each part of the fish, $S_1 \sim S_5$, $S_{fx}$, $S_{fy}$; and $\rho$ is the density of the fluid.

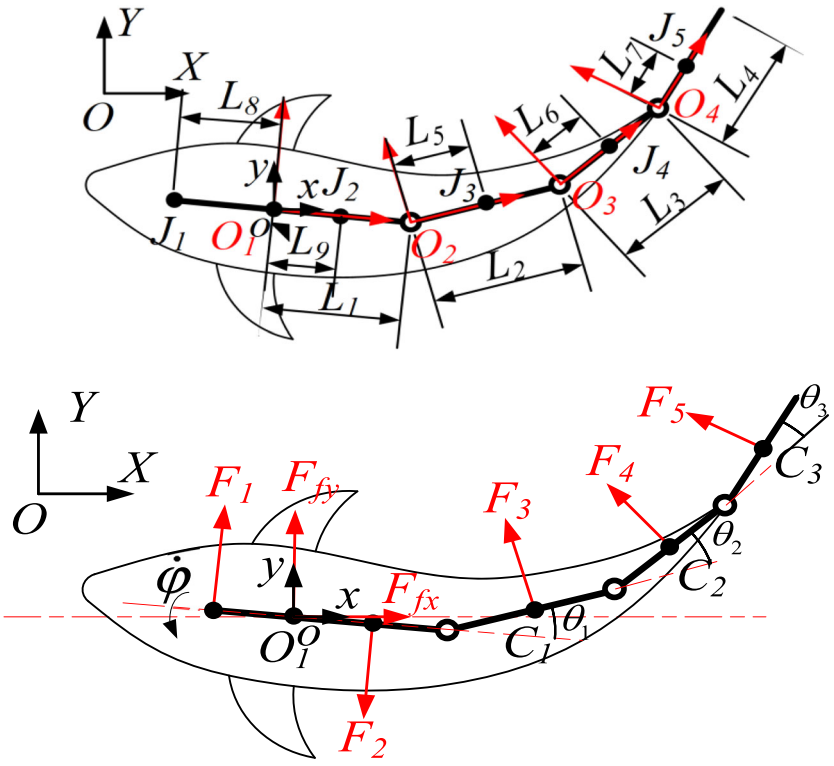


**Fig. 3** Coordinate systems and forces of bionic fish

Easy to know

$$v_{J_1} = \dot{\varphi} L_8 + v v_{J_2} = \dot{\varphi} L_9 + v \tag{4}$$

where $v = \left[\dot{x}\dot{y}0\right]^T$ is the actual speed of the bionic fish.

The coordinate systems of the caudal fin propulsion mechanism are shown in Fig. 4, and $v_{J3} \sim v_{J5}$ are calculated by coordinate transformation.

The transformation matrices between the coordinate systems of the bionic fish tail are as follows:

$${}^{i-1}T = \left[{}^{i-1}RP_iOI\right], {}^{i}T^{Ji+2} = \begin{bmatrix} I_{3\times3} & P_{Ji+2} \\ O & 1 \end{bmatrix} {}^{i-1}R = \begin{bmatrix} cos\theta_i & -sin\theta_i & 0 \\ sin\theta_i & cos\theta_i & 0 \\ 0 & 0 & 1 \end{bmatrix}$$

where ${}^{i}R^{i+1}$ is the rotation matrix, and $i = 1, 2, 3$, $P_1 = \boldsymbol{O}_{3\times1}$, $P_2 = [L_200]^T$, $P_3 = [L_300]^T$, $P_{J3} = [L_500]^T$, $P_{J4} = [L_600]^T$, $P_{J5} = [L_700]^T$, and $I_{3\times3}$ is the third-order unit matrix.

The velocities ${}^{i}v_{Ji}$ of the centroid $J_i$ of each part of the tail in the coordinate system $X_iO_iY_i$ are

$$\begin{aligned} {}^{1}v_{J3} &= {}^{1}R^{J3}\left[0L_5\dot{\theta}_10\right]^T {}^{2}v_{J4} \\ &= {}^{2}R^{J4}\left({}^{2}v_2 + \left[0 \;\; L_6\left(\dot{\theta}_1 + \dot{\theta}_2\right) \;\; 0\right]^T\right) {}^{3}v_{J5} \\ &= {}^{3}R^{J5}\left({}^{3}v_3 + \left[0 \quad L_7\left(\dot{\theta}_1 + \dot{\theta}_2 + \dot{\theta}_3\right) \quad 0\right]^T\right) \end{aligned} \tag{5}$$

The velocities ${}^{0}v_{Ji}$ of the centroid $J_i$ of each part of the tail in the base coordinate system $X_0O_0Y_0$ are

$${}^{0}v_{J3} = {}^{0}R^{J31}v_{J3}{}^{0}v_{J4} = {}^{0}R^{J42}v_{J4}{}^{0}v_{J5} = {}^{0}R^{J53}v_{J5} \tag{6}$$

where ${}^{0}R$ is

$${}^{0}R = \begin{bmatrix} cos\sum_{j=1}^{i-2}\theta_j & -sin\sum_{j=1}^{i-2}\theta_j & 0 \\ sin\sum_{j=1}^{i-2}\theta_j & cos\sum_{j=1}^{i-2}\theta_j & 0 \\ 0 & 0 & 1 \end{bmatrix}$$

where $i = 3, 4, 5$. The actual velocity on the centroid of each part of the tail is

$$v_{Ji} = {}^{0}v_{Ji} + v \tag{7}$$

The nonlinear dynamic model of the bionic fish can be obtained by Eq. (2) ~Eq. (7). To simplify the calculation, the following assumptions are made:

(1) Because only the low-speed movement of the bionic fish in a still water environment is considered, the influence of lateral velocity and centripetal force are ignored.
(2) In the swimming process of the bionic fish, the swing angle of the tail fluctuates, so the thrust generated by the tail swing also changes over time. For the convenience of calculation, the thrust generated by the tail is equivalent to a constant force through the principle of equal work in one cycle.

The work done by each part of the fish tail in the X direction and that in the Y direction in a tail swing cycle are as follows:

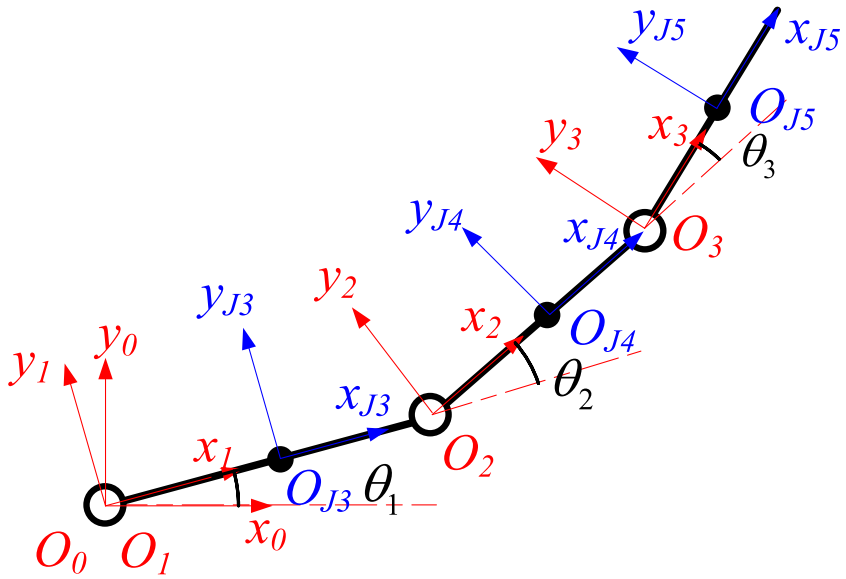


**Fig. 4** The coordinate systems of the caudal fin propulsion mechanism

$$\begin{aligned} W_{xi} &= \int_0^T F_{xi} v_{Ji} dt = v_{Ji} \int_0^T F_i sin\Theta_i dt \\ W_{yi} &= \int_0^T F_{yi} v_{Ji} dt = v_{Ji} \int_0^T F_i cos\Theta_i dt \end{aligned} \tag{8}$$

where $\Theta_i$ is the angle of each part of the tail. $F$ is the force generated by the tail swinging, and $T$ is the period of the tail swinging.

Let Eq. (8) satisfy Eq. (9):

$$\begin{aligned} v_{Ji} \int_0^T F_i sin\Theta_i dt &= v_{Ji} \int_0^T F_i k_i^x dt \\ v_{Ji} \int_0^T F_i cos\Theta_i dt &= v_{Ji} \int_0^T F_i k_i^y dt \end{aligned} \tag{9}$$

The equivalent parameters $k_i^x$ and $k_i^y$ can be obtained by Eq. (3), Eq. (7) and Eq. (9). Finally, the simplified nonlinear dynamic model of the bionic fish is

$$\begin{aligned} m\ddot{y} &= -\left[a_1 cHk_1^x k_1^y + \left(a_2 cHk_{\lambda_4}^x + a_3 cHk_{\lambda_1}^x\right) k_{\lambda_1}^y + a_4 cHk_{\lambda_2}^x k_{\lambda_2}^y\right] \dot{x}\omega \\ m\ddot{x} &= -\left[a_1 cH\left(k_1^x\right)^2 + \left(a_2 cHk_{\lambda_4}^x + a_3 cHk_{\lambda_1}^x\right) k_{\lambda_1}^x + a_4 cH\left(k_{\lambda_2}^x\right)^2\right] \dot{x}\omega \\ I_z\ddot{\varphi} &= -a_5 \dot{x}\dot{\varphi} - a_1 cH\left(L_1 - 0.5L_1 b^2 + L_5\right)\dot{x}\omega b \\ &\quad -\left(a_2 cH\lambda_4 + a_3 cH\lambda_1\right)\left[L_1 + L_2 + L_6 - \left(0.5L_1\lambda_1^2 + 0.5L_2 i_1^2\right)b^2\right]\dot{x}\omega b \\ &\quad -a_4 cH\lambda_2\left[L_1 + L_2 + L_3 + L_7 - \left(0.5L_1\lambda_2^2 + 0.5L_2\lambda_3^2 + 0.5L_3 i_2^2\right)b^2\right]\dot{x}\omega b \\ \dot{Y} &= \dot{x}\sin\varphi + \dot{y}\cos\varphi \\ \dot{X} &= \dot{x}\cos\varphi - \dot{y}\sin\varphi \end{aligned} \tag{10}$$

where $H$ is the rotation amplitude of the first joint of the caudal fin propulsion mechanism. $c$ is a constant in the derivation process, with $c = 2/\pi$.$a_1 \sim a_5$ and $\lambda_1 \sim \lambda_4$ are all constants,$a_1 = C_3 S_3 L_5 \rho$,$a_2 = C_4 S_4 L_2 \rho/2$,$a_3 = C_4 S_4 L_6 \lambda_1 \rho/2$, $a_4 = C_5 S_5 (L_2 + \lambda_1 L_3 + \lambda_2 L_7)\rho/2$, and $a_5 = (C_1\ S_1 L_8^2 + C_2\ S_2 L_9^2)\ \rho/2$.$\lambda_1 = 1 + i_1$, $\lambda_2 = 1 + i_1 + i_2$, $\lambda_3 = i_1 + i_2$, and $\lambda_4 = 1 + 2i_1$. $i_1$ and $i_2$ are the transmission ratios of each gear of the caudal propulsion mechanism.

## 3 Problem Formulation

### 3.1 CPG Model of the Bionic Fish

A central pattern generator (CPG) is a biological neural network that is widely found in vertebrates and invertebrates and can generate rhythm signals without sensory feedback [32]. Inspired by this, scholars have developed various CPG oscillator models, which are currently commonly used, including recursive neural oscillators, phase oscillators and Hopf oscillators [33–35]. This paper uses the Hopf oscillator as the basic unit of the CPG to construct the underlying motion control network. The mathematical model of the CPG network is

$$\begin{aligned} \dot{x_i} &= -\omega_i(\beta_i - b_i) + k\alpha_i\left(H_i^2 - \alpha_i^2 - (\beta_i - b_i)^2\right) \\ &\quad + h_i\left(\alpha_{i-1}\cos\phi_i + (\beta_{i-1} - b_{i-1})\sin\phi_{i,i-1}\right)\dot{y_i} \\ &= \omega_i\alpha_i + k(\beta_i - b_i)\left(H_i^2 - \alpha_i^2 - (\beta_i - b_i)^2\right) \\ &\quad + h_{i+1}\left(\alpha_{i+1}\sin\phi_{i+1} + (\beta_{i+1} - b_{i+1})\cos\phi_{i,i+1}\right) \end{aligned} \tag{11}$$

where $\alpha_i$ and $\beta_i$ are state variables of the $i$-th oscillator. $\omega_i$ and $H_i$ represent the oscillation frequency and amplitude of the $i$-th oscillator, respectively. $h_i$ and $\phi_i$ represent the coupling factor and phase difference of the $i$-th oscillator, respectively, and $b_i$ represents the offset of state variable $\beta_i$ in the $i$-th oscillator, with $i = 1, 2, 3$.

The CPG network constructed by coupling terms is shown in Fig. 5. The output signals of the CPG network are transmitted to the left pectoral fin, right pectoral fin and caudal fin of the bionic fish. The upper controller adjusts the frequency and offset of the CPG network in real time, and then, by changing the frequency and offset of the pectoral fin and caudal fin, the swimming speed and angular velocity are controlled, finally, the tracking control objective of the bionic fish is realized, that is, the actual state of the bionic fish satisfies the constraints of the reference trajectory in time and space, so as to ensure the smooth progress of the underwater operation task.

### 3.2 Design of the Model Predictive Controller

The motion control of the bionic fish is a kind of nonlinear problem with multiple constraints, and it needs to switch the swimming gait frequently during the trajectory tracking process to ensure tracking accuracy. Therefore, this paper uses the CPG network as the underlying motion controller to ensure smoothness in the motion control process. At the same time, model predictive control is introduced as the upper controller. The MPC and CPG are combined through the dynamic model of the bionic fish, and the MPC-CPG is developed. The parameters of the CPG network are adjusted in real time through the model predictive controller to complete the trajectory tracking task.

#### 3.2.1 Error Model

Eq. (10) shows that the system can be regarded as a control system with a control quantity $\boldsymbol{u}(\omega,\ b)$ and a state quantity $\boldsymbol{\chi}\left(\dot{y}, \dot{x}, \varphi, \dot{\varphi}, Y, X\right)$. Its general form is

$$\dot{\boldsymbol{\chi}} = f(\boldsymbol{\chi}, \boldsymbol{u}) \tag{12}$$

Each point on the given reference trajectory satisfies the above equation, the subscript $r$ is used to represent the reference quantity, and Eq. (12) becomes

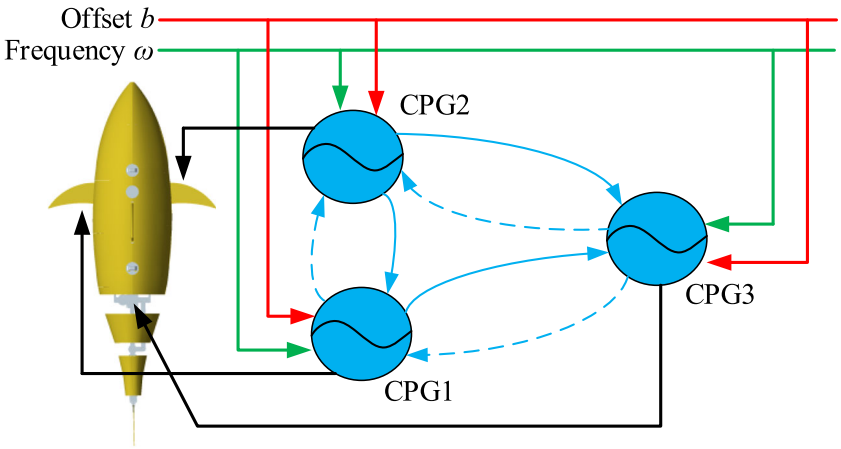


**Fig. 5** Bionic fish CPG network

$$\dot{\chi}_r = f(\chi_r, \boldsymbol{u}_r) \tag{13}$$

where $\chi_r = \left[\dot{y}_r\ \dot{x}_r\ \varphi_r\ \dot{\varphi}_r\ Y_r\ X_r\right]^T$ and $\boldsymbol{u}_r = [\omega_r b_r]^T$.

Expansion of Eq. (12) using a Taylor series at the reference trajectory point and ignoring higher-order terms yields

$$\dot{\chi} = f(\chi_r, \boldsymbol{u}_r) + \left.\frac{\partial f(\chi, \boldsymbol{u})}{\partial \chi}\right|_{\substack{\chi = \chi_r \\ \boldsymbol{u} = \boldsymbol{u}_r}} (\chi - \chi_r) + \left.\frac{\partial f(\chi, \boldsymbol{u})}{\partial \boldsymbol{u}}\right|_{\substack{\chi = \chi_r \\ \boldsymbol{u} = \boldsymbol{u}_r}} (\boldsymbol{u} - \boldsymbol{u}_r) \tag{14}$$

Subtracting (13) from (14), a linear error model can be obtained:

$$\dot{\tilde{\chi}} = \dot{\chi} - \dot{\chi}_r = \boldsymbol{A}(t)\tilde{\chi} + \boldsymbol{B}(t)\tilde{\boldsymbol{u}} \tag{15}$$

To apply this model to the design of model predictive controllers, Eq. (15) is discretized to obtain a discrete linear error model:

$$\tilde{\chi}(k+1) = \boldsymbol{A}_{k,t}\tilde{\chi}(k) + \boldsymbol{B}_{k,t}\tilde{\boldsymbol{u}}(k) \tag{16}$$

where $\boldsymbol{A}_{k,t} = I + T\boldsymbol{A}(t)$, $\boldsymbol{B}_{k,t} = T\boldsymbol{B}(t)$, and $T$ is the sampling time.

### 3.2.2 Cost Function

Referring to the method used in the literature [36], the MPC formulation for the bionic fish controller can be established as follows:

$$J(k) = \sum_{i=1}^{N_p} \left\| \boldsymbol{\eta}\left(k+i|t\right) - \boldsymbol{\eta}_r\left(k+i|t\right) \right\|_Q^2 + \sum_{i=1}^{N_c-1} \left\| \Delta \boldsymbol{U}\left(k+i|t\right) \right\|_R^2 \tag{17}$$

where $N_p$ is the prediction horizon and $N_c$ is the control horizon.

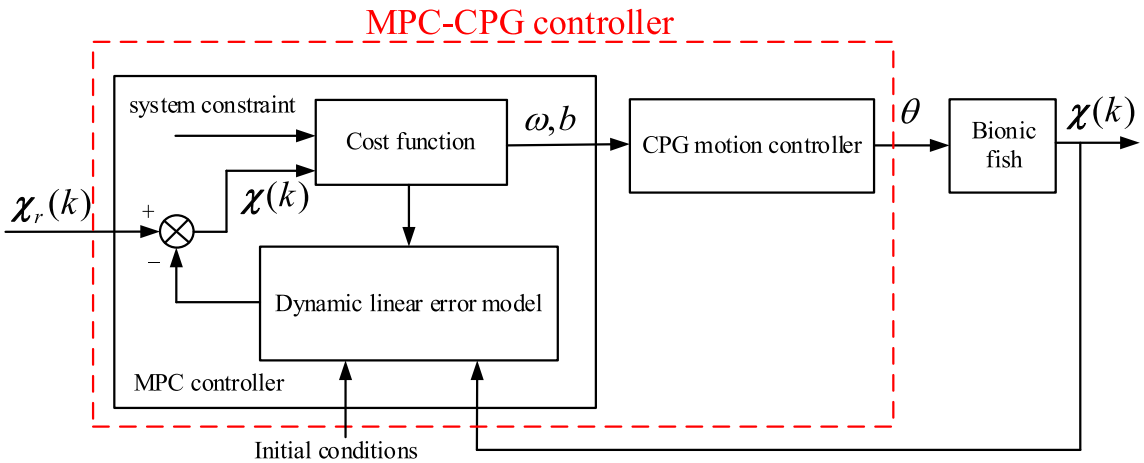


**Fig. 6** Control block diagram of MPC-CPG controller

**Table 2** Initial conditions and reference values of bionic fish

| | Reference trajectory$(x_r, y_r, \theta_r)$ | Initial error $(x_e, y_e, \theta_e)$ | Reference velocity $(u_r, \omega_r)$ |
|---|---|---|---|
| Circular | $(5cost, 5sint, t)$ | $(-2, 0, \pi/3)$ | $(0.25, 0.5)$ |
| Straight | $(t, 2, 0)$ | $(0, 1, 0)$ | $(0.25, 0)$ |

Eq. (16) is converted as follows:

$$\boldsymbol{\xi}(k|t) = \begin{bmatrix} \widetilde{\boldsymbol{\chi}}(k|t) \\ \widetilde{\boldsymbol{u}}(k-1|t) \end{bmatrix} \tag{18}$$

A new state space expression is obtained as follows:

$$\begin{aligned} \boldsymbol{\xi}(k+1|t) &= \widetilde{\boldsymbol{A}}_{k,t}\boldsymbol{\xi}(k|t) + \widetilde{\boldsymbol{B}}_{k,t}\Delta\boldsymbol{U}(k|t) \\ \boldsymbol{\eta}(k|t) &= \widetilde{\boldsymbol{C}}_{k,t}\boldsymbol{\xi}(k|t) \end{aligned} \tag{19}$$

where $\widetilde{\boldsymbol{A}}_{k,t} = \begin{bmatrix} \boldsymbol{A}_{k,t} & \boldsymbol{B}_{k,t} \\ \boldsymbol{0}_{m\times n} & \boldsymbol{I}_m \end{bmatrix}$, $\widetilde{\boldsymbol{B}}_{k,t} = \begin{bmatrix} \boldsymbol{B}_{k,t} \\ \boldsymbol{I}_m \end{bmatrix}$, $n$ is the dimension of the state quantity, and $m$ is the dimension of the control quantity.

After derivation, the predicted output expression of the system is obtained:

$$\boldsymbol{Y}(t) = \boldsymbol{\Psi}_t\boldsymbol{\xi}(t|t) + \boldsymbol{\Theta}_t\Delta\boldsymbol{U}(t) \tag{20}$$

where

$$Y(t) = \begin{bmatrix} \Delta u(t|t) \\ \Delta u(t+1|t) \\ \cdots \\ \Delta u(t+N_c|t) \end{bmatrix} \Psi_t = \begin{bmatrix} \widetilde{C}_{t,t}\widetilde{A}_{t,t} \\ \widetilde{C}_{t,t}\widetilde{A}_{t,t}^2 \\ \cdots \\ \widetilde{C}_{t,t}\widetilde{A}_{t,t}^{N_c} \\ \cdots \\ \widetilde{C}_{t,t}\widetilde{A}_{t,t}^{N_p} \end{bmatrix}$$

$$\Theta_t = \begin{bmatrix} \widetilde{C}_{t,t}\widetilde{B}_{t,t} & 0 & 0 & 0 \\ \widetilde{C}_{t,t}\widetilde{A}_{t,t}\widetilde{B}_{t,t} & \widetilde{C}_{t,t}\widetilde{B}_{t,t} & 0 & 0 \\ \vdots & & \ddots & \vdots \\ \widetilde{C}_{t,t}\widetilde{A}_{t,t}^{N_c-1}\widetilde{B}_{t,t} & \widetilde{C}_{t,t}\widetilde{A}_{t,t}^{N_c-2}\widetilde{B}_{t,t} & \cdots & \widetilde{C}_{t,t}\widetilde{B}_{t,t} \\ \widetilde{C}_{t,t}\widetilde{A}_{t,t}^{N_c}\widetilde{B}_{t,t} & \widetilde{C}_{t,t}\widetilde{A}_{t,t}^{N_c-1}\widetilde{B}_{t,t} & \cdots & \widetilde{C}_{t,t}\widetilde{A}_{t,t}\widetilde{B}_{t,t} \\ \vdots & & \ddots & \vdots \\ \widetilde{C}_{t,t}\widetilde{A}_{t,t}^{N_p-1}\widetilde{B}_{t,t} & \widetilde{C}_{t,t}\widetilde{A}_{t,t}^{N_p-2}\widetilde{B}_{t,t} & \cdots & \widetilde{C}_{t,t}\widetilde{A}_{t,t}^{N_p-N_c-1}\widetilde{B}_{t,t} \end{bmatrix}, \Delta U(t) = \begin{bmatrix} \Delta u(t|t) \\ \Delta u(t+1|t) \\ \cdots \\ \Delta u(t+N_c|t) \end{bmatrix}$$

Substituting Eq. (20) into Eq. (17), the cost function in its complete form can be obtained.

**Table 3** Parameter setting

| Parameter | | Numerical value |
|---|---|---|
| MPC | Prediction step $N_p$ | 5 |
| | Control step $N_c$ | 3 |
| | Sampling time $T$ | 0.5 |
| CPG | Amplitude $H_i$ | 10 |
| | Phase difference $\phi_i$ | $\pi$ |
| | Coupling factor $h_i$ | 0.5 |
| | Convergence factor $k$ | 15 |

The expression form of the control quantity constraint and the control increment constraint during the movement of the bionic fish are as follows:

$$\begin{aligned} &\boldsymbol{u}_{\min}(t+k) \leqslant \boldsymbol{u}(t+k) \leqslant \boldsymbol{u}_{\max}(t+k) \\ &\Delta\boldsymbol{u}_{\min}(t+k) \leqslant \Delta\boldsymbol{u}(t+k) \leqslant \Delta\boldsymbol{u}_{\max}(t+k) \end{aligned}, k = 0, 1, \cdots, N_c-1 \tag{21}$$

The constraints are combined into matrix form as

$$\boldsymbol{U}_{\min} \leqslant \boldsymbol{K}\Delta\boldsymbol{U}_t + \boldsymbol{U}_t \leqslant \boldsymbol{U}_{\max} \tag{22}$$

where $\boldsymbol{U}_{\min}$ and $\boldsymbol{U}_{\max}$ are the minimum and maximum values of the control variable in the control horizon, respectively. $\boldsymbol{U}_t = \boldsymbol{1}_{N_c} \otimes \boldsymbol{u}(k-1)$, $\boldsymbol{1}_{N_c}$ is the column vector with $N_c$ rows, and $\otimes$ is the Kronecker product.

$$\boldsymbol{K} = \begin{bmatrix} 1 & 0 & \cdots & 0 \\ 1 & 1 & 0 & 0 \\ \vdots & \vdots & \ddots & \vdots \\ 1 & 1 & \cdots & 1 \end{bmatrix}_{N_c\times N_c} \otimes \boldsymbol{I}_m \tag{23}$$

### 3.2.3 Stability Proof

In this paper, Lyapunov's second method is used to prove the stability, and the optimal cost function at time $k$ is selected as the Lyapunov function, that is, $minJ(k) = J^*(k) = V^*(k)$. If the Lyapunov function satisfies $V^*(k+1) \leq V^*(k)$ at time $k+1$, the system is stable.

$$V^*(k) = min\left\{ \sum_{i=1}^{N_p} \|\eta(k) - \eta_r(k)\|_Q^2 + \sum_{i=0}^{N_c-1} \|\Delta u(k)\|_R^2 \right\} \tag{24}$$

Obviously, the selected Lyapunov function in Eq. (24) is $V^*(k) = 0$ when $k = 0$ and $V^*(k) > 0$ when $k \neq 0$. The optimal control quantity $\widetilde{u}(k+1+i|k+1)$ and the optimal control increment $\Delta\widetilde{u}(k+1+i|k+1)$ of the system are as follows:

$$\begin{aligned} \widetilde{u}(k+1+i|k+1) &= \left[\widetilde{u}(k+1|k+1), \widetilde{u}(k+2|k+1), \ldots, \widetilde{u}(k+N_c|k+1)\right] \\ &= \left[\widetilde{u}^*(k+1|k), \widetilde{u}^*(k+2|k), \ldots, \widetilde{u}^*(k+N_c|k)\right] \\ \Delta\widetilde{u}(k+1+i|k+1) &= \left[\Delta\widetilde{u}(k+1|k+1), \Delta\widetilde{u}(k+2|k+1)\ldots, \Delta\widetilde{u}(k+N_c|k+1)\right] \\ &= \left[\Delta\widetilde{u}^*(k+1|k), \Delta\widetilde{u}^*(k+2|k), \ldots, \Delta\widetilde{u}^*(k+N_c|k)\right] \end{aligned} \tag{25}$$

According to Eq. (25), $J(k+1)$ and $V^*(k)$ have the following relationship:

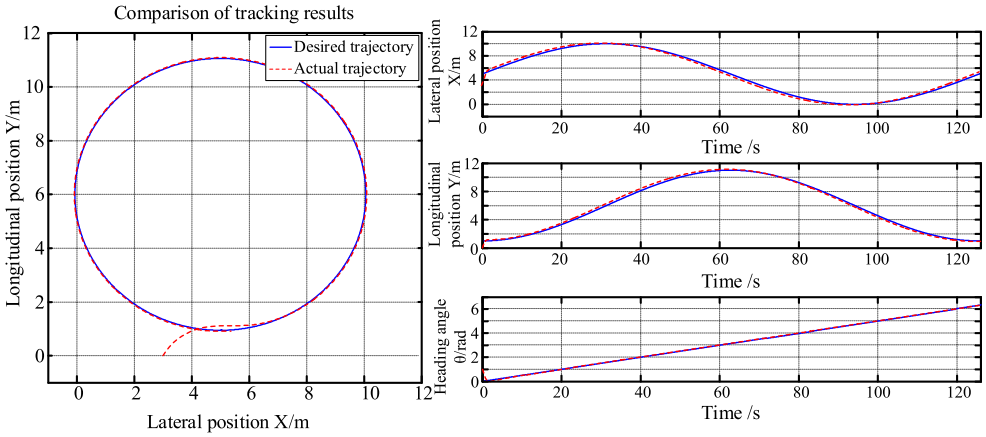


(a) Trajectory tracking

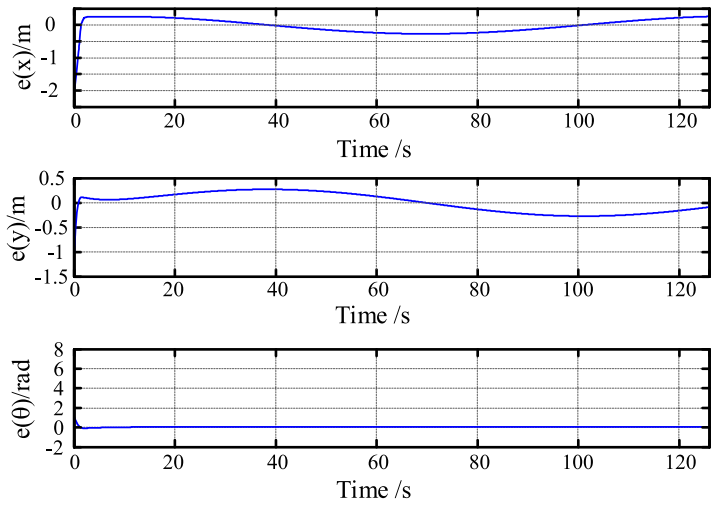


(b) Tracking error

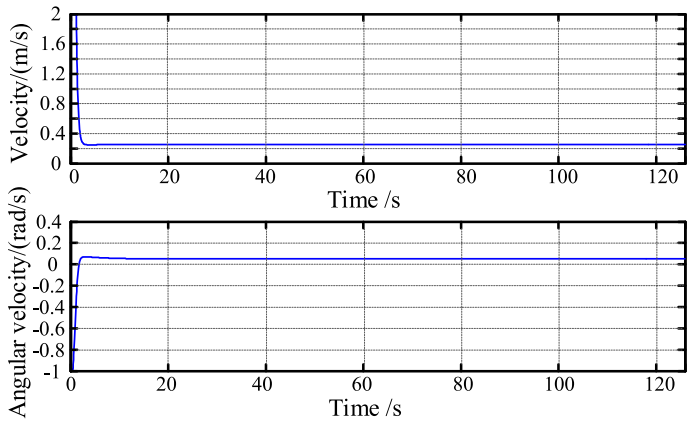


(c) Velocity and angular velocity

**Fig. 7** Simulation results of circular trajectory tracking

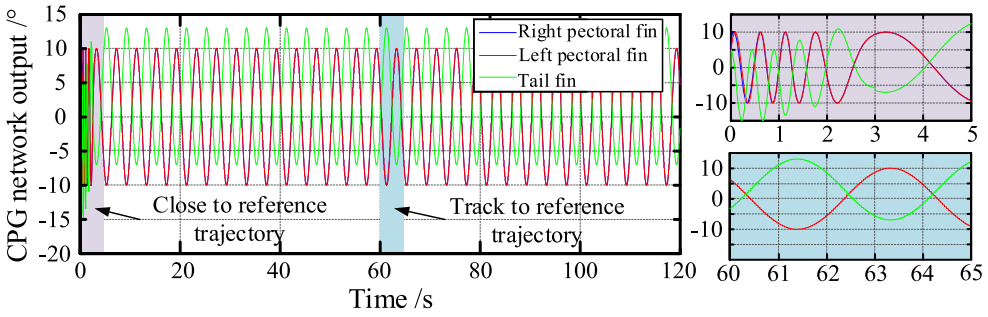


**Fig. 8** Output signals of CPG network of circular trajectory tracking

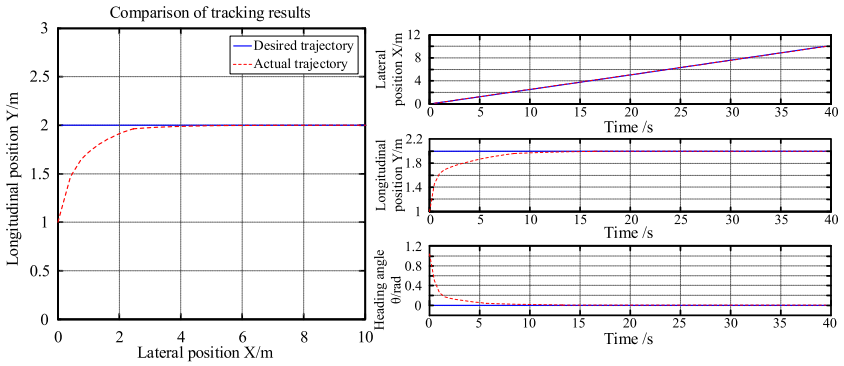


(a) Trajectory tracking

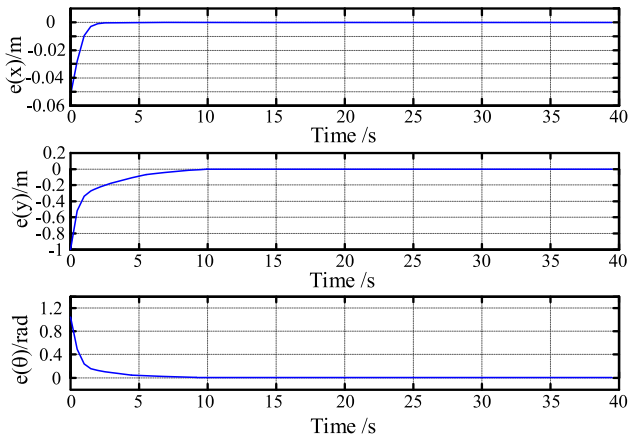


(b) Tracking error

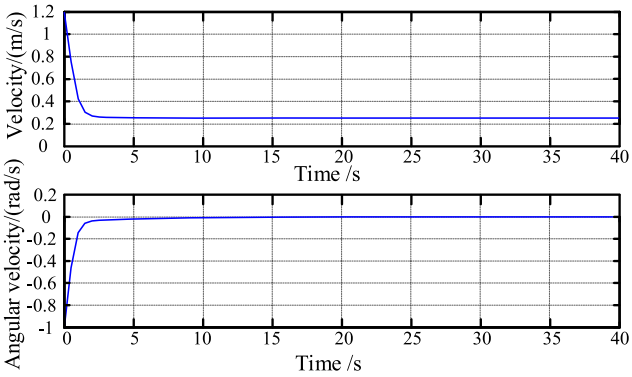


(c) Velocity and angular velocity

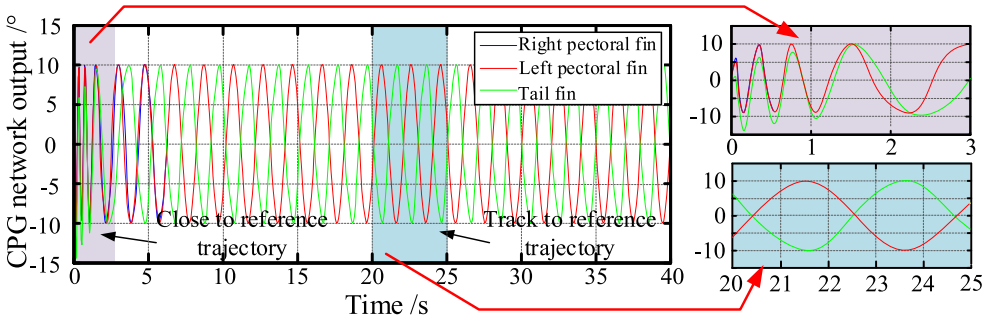


**Fig. 10** Output signals of CPG network of straight trajectory tracking

$$
\begin{aligned}
J(k+1) &= \sum_{i=1}^{N_p} \|\eta(k+1+i|k+1)-\eta_r(k+1+i|k+1)\|_Q^2 \\
&\quad + \sum_{i=0}^{N_c-1} \|\Delta u(k+1+i|k+1)\|_R^2 \\
&= \sum_{i=1}^{N_p} \left\|\eta^*(k+1+i|k)-\eta_r(k+i|k)\right\|_Q^2 + \sum_{i=1}^{N_c-1} \left\|\Delta u^*(k+i|k)\right\|_R^2 \\
&= \sum_{i=1}^{N_p} \left\|\eta^*(k+1+i|k)-\eta_r(k+i|k)\right\|_Q^2 + \sum_{i=1}^{N_c-1} \left\|\Delta u^*(k+i|k)\right\|_R^2 \\
&\quad -\|\eta(k|k)-\eta_r(k|k)\|_Q^2 - \left\|\Delta u^*(k|k)\right\|_R^2 \\
&= V^*(k) - \|\eta(k|k)-\eta_r(k|k)\|_Q^2 - \|\Delta u(k|k)\|_R^2
\end{aligned}
\tag{26}
$$

In addition, because $V^*(k+1)$ is the optimal solution to the cost function, $V^*(k+1) \le J(k+1)$. According to Eq. (26), we obtain

$$
V^*(k+1) \le J(k+1) \le V^*(k) - \left\|\eta^*(k)-\eta_r(k)\right\|_Q^2 - \left\|\Delta u^*(k)\right\|_R^2 \tag{27}
$$

Because $\|\eta^*(k)-\eta_r(k)\|_Q^2$ and $\|\Delta u^*(k)\|_R^2$ are not negative, the following can be obtained

$$
V^*(k+1) \le V^*(k) \tag{28}
$$

Thus, the stability of the system is proven.

## 4 Simulation and Experiment

A block diagram of the MPC-CPG controller is shown in Fig. 6. The model predictive controller calculates the control quantity at the next moment according to the error between the reference trajectory and the actual trajectory at the current time. The control quantity is input to the CPG network in the form of a CPG parameter for adjustment, and then, the CPG outputs the control signals for the pectoral fins and caudal fin of the bionic fish. This process is continuously loop, and finally, the trajectory tracking task is completed.

To verify the effectiveness of the designed controller, in this paper, simulations and experiments are carried out on tracking the circular trajectory and straight trajectory of the bionic fish. The initial conditions and reference values are shown in Table 2. The parameter settings of the MPC and CPG are shown in Table 3.

In the simulation process, the control quantity constraint and control increment constraint of the model predictive controller are as follows

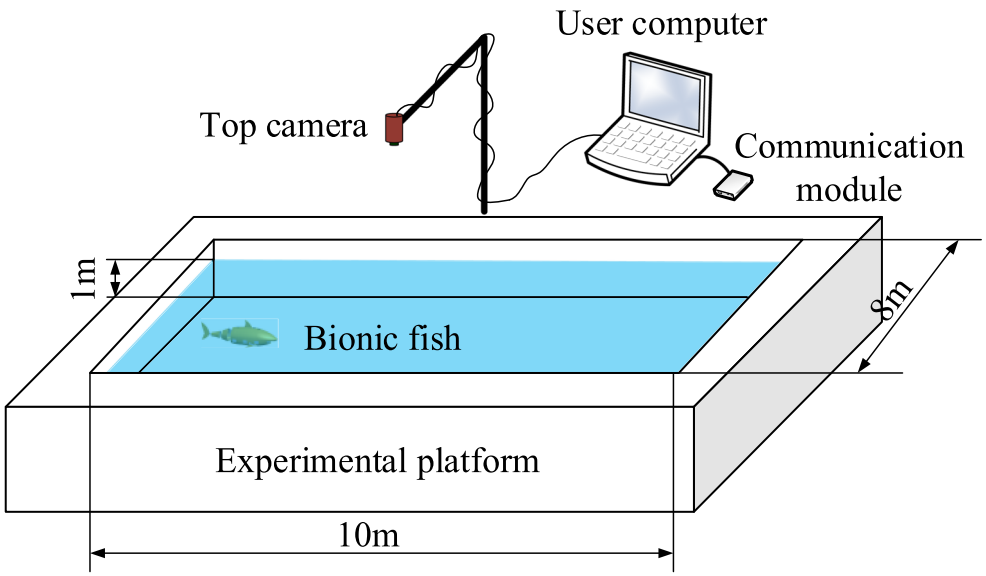


**Fig. 11** Experimental platform

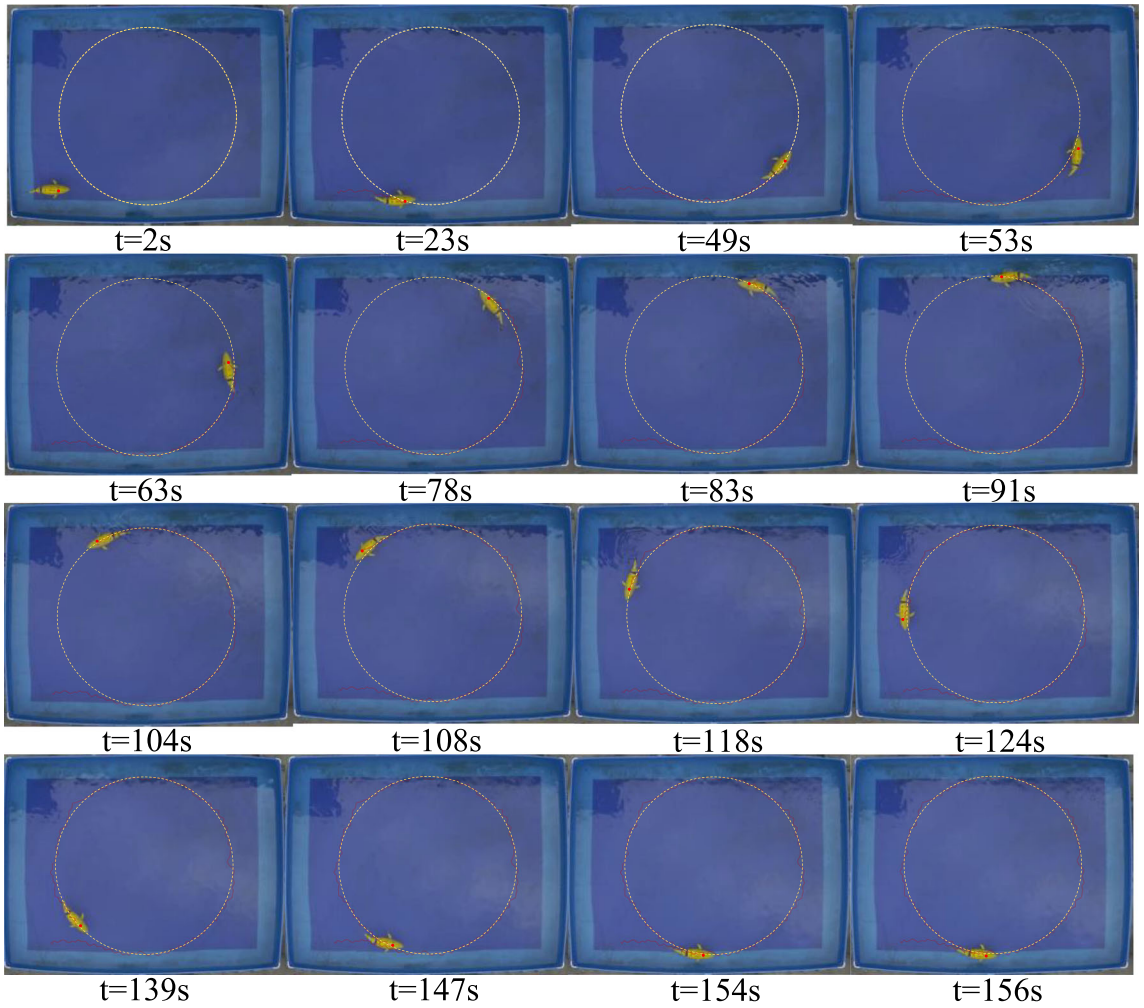


**Fig. 12** Circular trajectory tracking experiment

$$\begin{bmatrix} -4\pi \\ -5 \end{bmatrix} \leq \begin{bmatrix} \omega \\ b \end{bmatrix} \leq \begin{bmatrix} 4\pi \\ 5 \end{bmatrix} \\ \begin{bmatrix} -0.1\pi \\ -0.5 \end{bmatrix} \leq \begin{bmatrix} \Delta\omega \\ \Delta b \end{bmatrix} \leq \begin{bmatrix} 0.1\pi \\ 0.5 \end{bmatrix} \tag{29}$$

The simulation results of the circular trajectory tracking task are shown in Fig. 7. Figure 7(a) it shows that the model predictive controller quickly eliminated the position error and the heading angle error of the bionic fish and smoothly tracked the reference trajectory in 2 s, and the tracking effect is good. Figure 7(b) shows that the position error is always kept at −0.27 m ~ 0.27 m (−15.5% ~ 15.5% of the body length), and the heading angle error converges to 0 after 2 s. Figure 7(c) shows that when the bionic fish starts to move, to track the reference trajectory as soon as possible, the velocity and angular velocity are relatively large. As the tracking error decreases, the velocity and angular acceleration also decrease and finally stabilize at the reference value. Correspondingly, the outputs of the CPG network during the trajectory tracking process are shown in Fig. 8. The figure shows that the oscillation frequency of the CPG network is relatively large in the beginning, which makes the caudal fin of the bionic fish swing at a relatively large frequency, thus quickly approaching the reference trajectory and eliminating the tracking error. The offset of the CPG is gradually reduced from −5° to 0° and then is gradually increased. After tracking the reference trajectory, the frequency of the CPG stabilizes at 0.5π, and the offset stabilizes at 3°.

The simulation results of straight trajectory tracking are shown in Fig. 9. The figure shows that the position error and heading angle error of the bionic fish are quickly eliminated by the model predictive controller. After 10 s, the reference trajectory is tracked, and the position error and the heading angle error both converge to 0. Correspondingly, the output of the CPG network in the trajectory tracking process is shown in Fig. 10. Similar to tracking the circular trajectory, the oscillation frequency of the CPG network is relatively large in the beginning so that the bionic fish quickly approaches the reference trajectory and tracking errors are eliminated. The offset of the CPG gradually decreases from −5°, the offset stabilizes at 0° after tracking the reference trajectory, and the frequency of the CPG is stable at 0.5π.

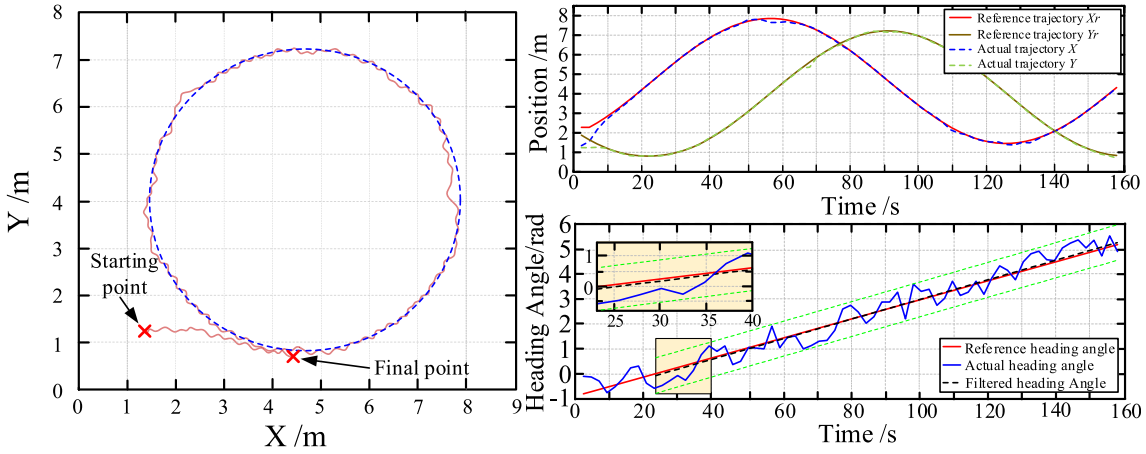


(a) Trajectory tracking

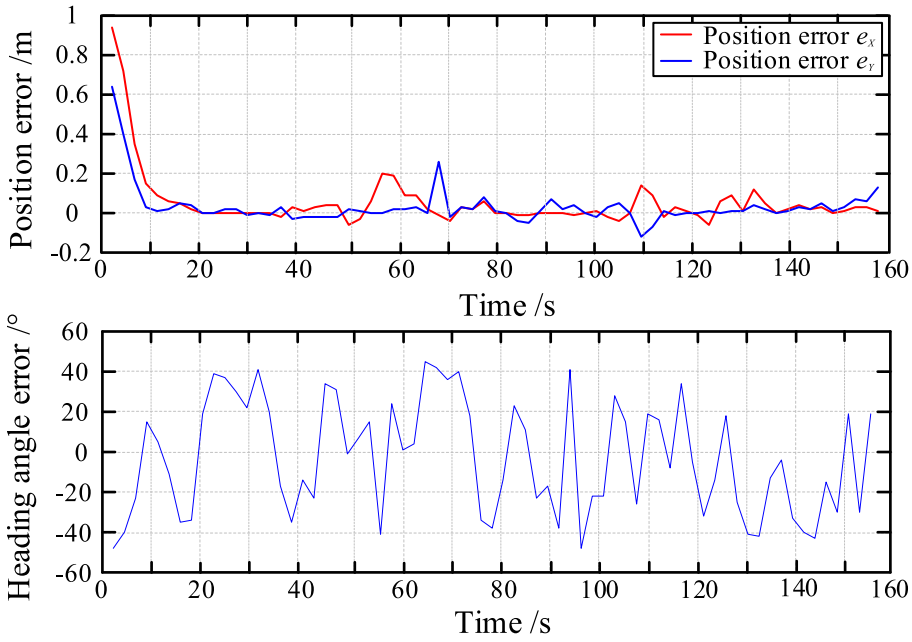


(b) Tracking error

**Fig. 13** Experimental results of circular trajectory tracking

The simulation results show that with the adjustment of the MPC-CPG, the system can quickly eliminate the position and heading angle errors so that the system can quickly reach a stable state, and the system has good dynamic characteristics in the process of reaching the steady state.

Compared with the method in reference [37], the control method proposed in this paper has obvious advantages based on three aspects: tracking accuracy, motion performance and handling of constraints. First, reference [37] used a type 1 servo control (T1SC) with an LQR optimal state feedback technique in the trajectory tracking control of bionic fish, and the tracking accuracy of the simulation experiment (−32% ~ 32% of the body length) was lower than that of the method presented in this paper. Second, reference [37] sent the joint rotation angle value calculated by dynamics directly to the drive motor. Compared with the CPG control method, this method has shortcomings in the smoothness and coordination of motion control. In addition, reference [37] only considered the variation in the offset of the fish tail swing, while this paper also considers the variation in the offset and frequency of the fish tail swing, achieving better flexibility. Finally, although reference [37] used LQR to obtain optimal control, it did not incorporate many of the constraints of the motion control of bionic fish into the control process, and the problem of driver oversaturation is prone to occur. The MPC used in this paper can solve this kind of problem well.

To further verify the effectiveness of the MPC-CPG, experimental verification is carried out based on the simulation. As shown in Fig. 11, the experimental platform mainly includes a pool with a length of 10 m, a width of 8 m, and a depth of 1 m, a top camera, a user computer, and a communication module. Under static water conditions, experiments were carried out on, tracking the circular trajectory and straight trajectory of the bionic fish. In the experiment, a marking point was set on the back of the bionic fish. During the swimming process, the computer recorded the actual swimming trajectory of the bionic fish through the top camera.

The experimental process of circular trajectory tracking is shown in Fig. 12. The yellow dotted line represents the reference trajectory, which is a circular trajectory with a diameter of 6.5 m, and the red line represents the actual trajectory of the moving bionic fish. At 2 s, the bionic fish starts to swim under the condition of initial error, and then, under the control of the MPC-CPG controller, the error with the reference trajectory is continuously reduced. At 23 s, it tracks the reference trajectory and continues to swim along the reference trajectory. Finally, the tracking of the entire circular trajectory is completed after 154 s. During the entire tracking process, the bionic fish smoothly approaches and tracks the reference trajectory.

The experimental results of circular trajectory tracking are shown in Fig. 13. The figure shows that the initial position errors in the X and Y directions are 0.94 m and 0.64 m, respectively. The position errors in the X and Y directions gradually decrease as the bionic fish swims. At 23 s, the bionic fish tracks the reference trajectory, and then, it continues to swim along the reference trajectory, finally completing the trajectory tracking task. The position error in the X and Y directions is always kept at −0.12 m ~ 0.26 m; that is, the position error is always kept at −6.9% ~ 14.9% of the body length. Due to the unique movement mode of the bionic fish, its head is always in a state of swinging during swimming. Therefore, the actual heading angle of the bionic fish when swimming always fluctuates around the reference heading angle, and the fluctuation range is −48° ~ 45°. The error between the filtered heading angle and the reference heading angle is kept at −4.76° ~ 4.73°, so the bionic fish has good heading angle tracking performance in the trajectory tracking process.

The experimental process of straight trajectory tracking is shown in Fig. 14. The figure shows that the bionic fish tracked the reference trajectory at 33 s and continued to swim along the reference trajectory. Finally, tracking of the entire straight trajectory is completed after 63 s. During the whole tracking process, the bionic fish can smoothly approach and track the reference trajectory.

The experimental results of straight trajectory tracking are shown in Fig. 15. The figure shows that the initial position errors in the X and Y directions are 0 m and 4 m, respectively. The position errors in the X and Y directions gradually decrease as the bionic fish swims. At 33 s, the bionic fish tracks the reference trajectory, and then, the position error in the X and Y directions is always kept at −0.15 m ~ 0.15 m; that is, the position

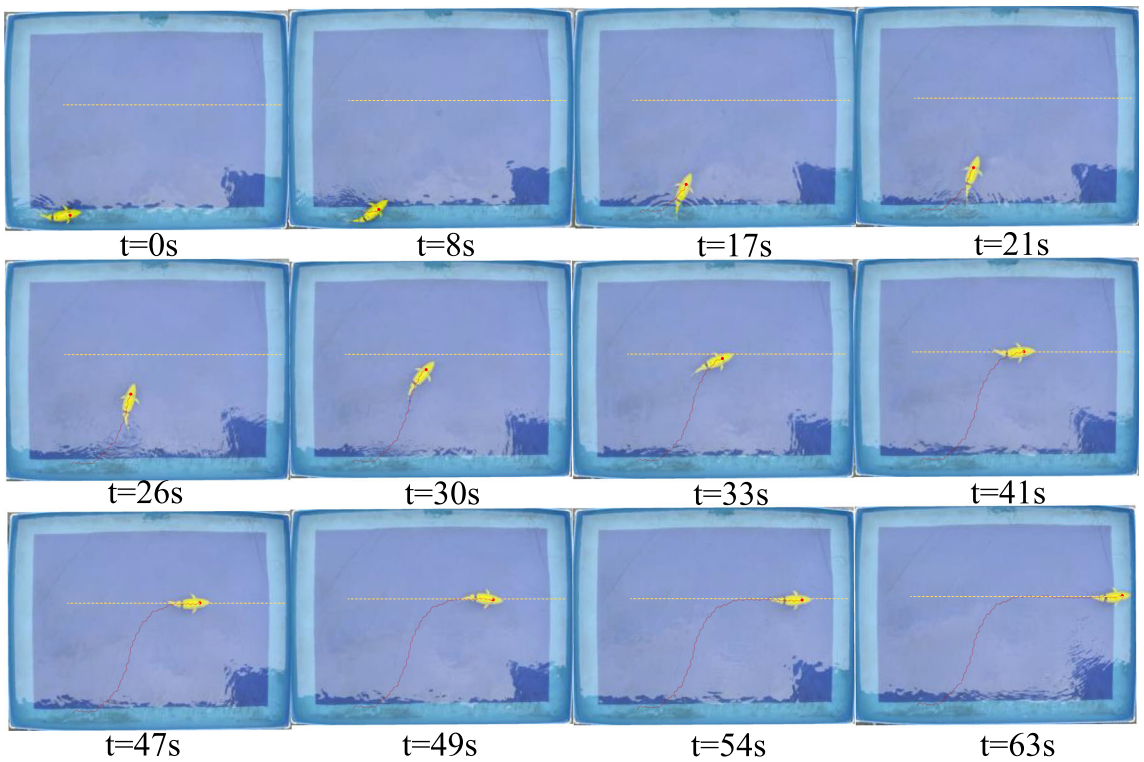


**Fig. 14** Straight trajectory tracking experiment

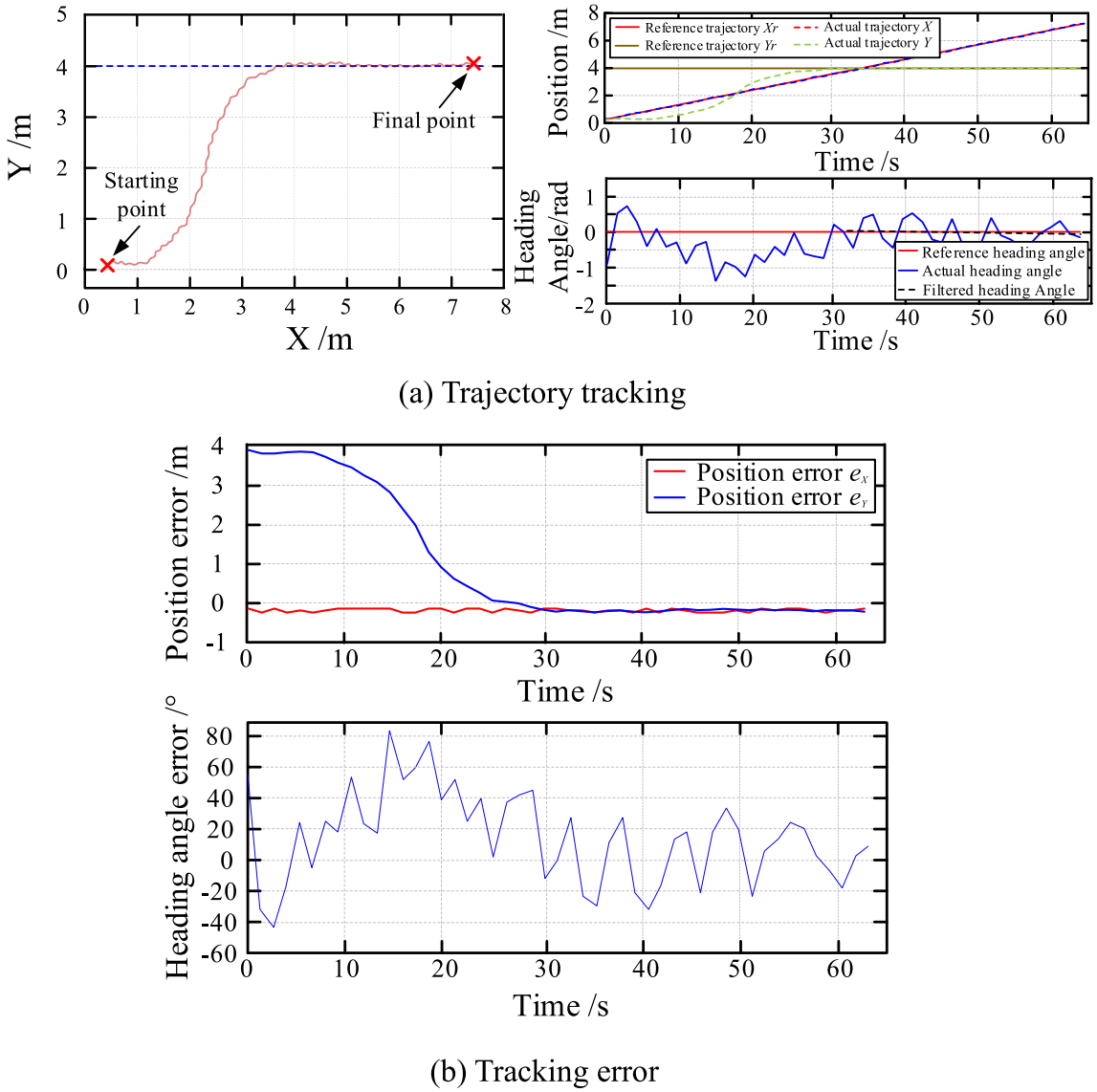


**Fig. 15** Experimental results of straight trajectory tracking

error is always kept at −8.6% ~ 8.6% of the body length. The error between the filtered heading angle and the reference heading angle is maintained at −3.24° ~ 3.55°, so the bionic fish has a good heading angle tracking performance in the trajectory tracking process.

Compared with the simulation results, during the experiment, the error between the actual motion trajectory and the reference trajectory always fluctuates within a small range. On the one hand, when the bionic fish swims, its head sways due to the swing of its tail, which causes the mark on its head to fluctuate near the reference trajectory and results in errors. This error can be improved by reducing the amplitude of head shaking, but it cannot be eliminated. On the other hand, because the pool is not completely static, the bionic fish is subjected to some external disturbances during swimming.

Compared with the method in reference [38], the control method proposed in this paper has obvious advantages from three aspects: tracking accuracy, smoothness of drive control and handling of constraints. First, reference [38] used a method based on optical flow target detection and a PID for tracking control of bionic fish, and the tracking accuracy of the prototype experiment (−28.7% ~ 28.7% of the body length) was lower than that of the method in this paper. Second, reference [38] used the method of multilink fitting fish body waves to control the swing of fish tails. Compared with the CPG control method adopted in this paper, it has shortcomings in terms of mobility and flexibility. Finally, similar to reference [37], reference [38] used a PID as the tracking controller, which cannot incorporate many constraints of the motion control of the bionic fish into the control process, and the problem of driver oversaturation is also prone to occur.

Therefore, the experiment shows that the bionic fish shows good tracking trajectory performance, which further verifies the effectiveness of the MPC-CPG proposed in this paper.

## 5 Conclusions

Based on the nonlinear dynamics model of bionic fish, this paper establishes a model predictive controller and then combines the model predictive controller with a CPG to propose an MPC-CPG for bionic fish trajectory tracking control. The nonlinear dynamic model of the bionic fish is established by Newton-Euler equations and D-H coordinate transformation. The MPC-CPG is composed of an upper MPC and a lower CPG network. The model predictive controller directly adjusts the parameters of the CPG network according to the error of the actual trajectory and the reference trajectory and then adjusts the motion mode through the CPG network to realize the trajectory tracking of the bionic fish. The entire control structure provides stable, adaptable and smooth gait transitions according to environmental changes. Finally, experiments are conducted to verify the tracking performance of the MPC-CPG on the circular trajectory and straight trajectory. The experiment shows that under the condition of initial error, the bionic fish can quickly eliminate position error and heading angle error and track the reference trajectory. The effectiveness of the proposed MPC-CPG for tracking control of the bionic fish trajectory is verified.

**Code or Data Availability** Available.

**Authors' Contributions** Zheping Yan: Conceptualization, Methodology, Resources.
Haoyu Yang: Methodology, Validation, Writing - Original Draft.
Wei Zhang: Conceptualization, Resources.
Qingshuo Gong: Software, Validation, Visualization.
Fantai Lin: Software, Validation, Visualization.
Yu Zhang: Software, Validation, Visualization.

**Funding** This work was supported by National Natural Science Foundation of China (No.51679057), National Nature Science Foundation of China under Grant (No.51609046, E1102/52071108) and Defense Technology and Industry Agency stabilization Support Program (JCKYS2020SXJQR-04).

## Declarations

**Ethics Approval** Approvals.

**Consent to Participate** All the authors of this article agreed to participate.

**Consent for Publication** All authors of this article agree to publish.

**Conflicts of Interest/Competing Interests** The authors declare that they have no known competing financial interests or personal relationships that could have appeared to influence the work reported in this paper.

## References

1. Katzschmann, R.K., Delpreto, J.J., Maccurdy, R., Rus, D.L.: Exploration of underwater life with an acoustically controlled soft robotic fish. Sci. Robot. **3**(16), eaar3449 (2018)
2. Yu, J., Yuan, J., Wu, Z., Min, T.: Data-driven dynamic modeling for a swimming robotic fish. IEEE Trans. Ind. Electron. **63**(9), 5632–5640 (2016). https://doi.org/10.1109/TIE.2016.2564338
3. Wang, J., Wu, Z., Tan, M., Yu, J.: 3-D path planning with multiple motions for a gliding robotic dolphin. IEEE Trans. Syst., Man, Cybern., Syst. **51**(5), 2904–2915 (2019)
4. Dong, H.J., Wu, Z.X., Chen, D., Tan, M., Yu, J.Z.: Development of a whale shark-inspired gliding robotic fish with high maneuverability. IEEE-ASME Trans. Mechatron. **25**(6), 2824–2834 (2020)
5. Fu, S., Wei, F., Yin, C., Yao, L., Wang, Y.: Biomimetic soft microswimmers: from actuation mechanisms to applications. Biomed. Microdevices. **23**(1), 6 (2021)
6. Duraisamy, P., Sidharthan, R.K., Santhanakrishnan, M.N.: Design, modeling, and control of biomimetic fish robot: a review. J. Bionic Eng. **16**(6), 967–993 (2019)
7. Xie, F., Zuo, Q., Chen, Q., Fang, H., He, K., Du, R.: Designs of the Biomimetic Robotic Fishes Performing Body and/or Caudal Fin (BCF) Swimming Locomotion: A Review. J. Intell. Robot. Syst. **102**(1), (2021). https://doi.org/10.1007/s10846-021-01379-1
8. Fu, S., Wei, F., Yin, C., Yao, L., Wang, Y.: Biomimetic soft microswimmers: from actuation mechanisms to applications. Biomed. Microdevices. **23**(6), 6 (2021)
9. Yaowei, W., Zhijian, J., Haichuan, Z.: J. Intell. Syst. **9**(3), 276–284 (2014)
10. Chen, Z.: Pneumatic Net Due Fish Body Wave Motion and the Research of Actuator Implementation [D]. Hunan University, (2020)
11. Yu, J.Z., Li, W., Ren, Z.Y.: A survey on fabrication, control, and hydrodynamic function of biomimetic robotic fish. Sci China Technol Sci. **60**(9), 1365–1380 (2017)
12. Deniz, K., Ozmen, K.G., Guoyuan, L., Cafer, B., Mustafa, A., Hakan, A.Z.: Locomotion control of a biomimetic robotic fish based on closed loop sensory feedback CPG model. J. Mar. Eng. Technol. **20**(2), 125–137 (2021)
13. Cafer, B., Gonca, O.K., Deniz, K., Hakan, A.Z., Mustafa, A.: CPG-based autonomous swimming control for multi-tasks of a biomimetic robotic fish [J]. Ocean Eng. **189**(C), 106334 (2019). https://doi.org/10.1016/j.oceaneng.2019.106334
14. Knuesel, J., Crespi, A., Cabelguen, J.-M., Ijspeert, A.J., Ryczko, D.: Reproducing Five Motor Behaviors in a Salamander Robot With Virtual Muscles and a Distributed CPG Controller Regulated by Drive Signals and Proprioceptive Feedback. Front. Neurorobot. **14**, 604426 (2020)
15. Chen, J.Y., Yin, B., Wang, C.C., Xie, F.R., Du, R.X., Zhong, Y.: Bioinspired closed-loop CPG-based control of a robot fish for obstacle avoidance and direction tracking. J. Bionic Eng. **18**(1), 171–183 (2021). https://doi.org/10.1007/s42235-021-0008-0
16. Cao, Y., Lu, Y., Cai, Y.R., Bi, S.S., Pan, G.: CPG-fuzzy-based control of a cownose-ray-like fish robot. Ind. Robot: The International Journal of Robotics Research and Application. **46**(6), 779–791 (2019). https://doi.org/10.1108/IR-02-2019-0029
17. Wang, G., Chen, X., Han, S.-K.: Central pattern generator and feedforward neural network-based self-adaptive gait control for a crab-like robot locomoting on complex terrain under two reflex

mechanisms [J]. Int. J. Adv. Robot. Syst. **14**(4), (2017). https://doi.org/10.1177/1729881417723440
18. Bing, Z.S., Cheng, L., Chen, G., Rohrbein, F., Huang, K., Knoll, A.: Towards autonomous locomotion: CPG-based control of smooth 3D slithering gait transition of a snake-like robot. Bioinspir. Biomim. **12**(3), 1–16 (2017). https://doi.org/10.1088/1748-3190/aa644c
19. Yu, J., Wu, Z., Wang, M., Tan, M.: CPG network optimization for a biomimetic robotic fish via PSO. IEEE Trans. Neural Netw. Learn. Syst. **27**(9), 1962–1968 (2016). https://doi.org/10.1109/TNNLS.2015.2459913
20. Wang, M., Dong, H., Li, X., et al.: Control and Optimization of a Bionic Robotic Fish Through a Combination of CPG model and PSO [J]. Neurocomputing. **14**(4), 144152 (2019)
21. Wang, Y., Xue, X.H., Chen, B.F.: Matsuoka's CPG with desired rhythmic signals for adaptive walking of humanoid robots. IEEE Trans. Cybern. **50**(2), 613–626 (2020). https://doi.org/10.1109/TCYB.2018.2870145
22. Yu, H., Guo, C., Yan, Z.: Globally finite-time stable three-dimensional trajectory tracking control of underactuated UUVs. Ocean Eng. **109**, 106329 (2019)
23. Yanbin, T.: Research on UUV Recovery Control Method of Moving Pedestal Based on Model Predictive Control [D]. Harbin engineering university, (2020)
24. Yang, C., Yao, F., Zhang, M.: Adaptive Backstepping Terminal Sliding Mode Control Method Based on Recurrent Neural Networks for Autonomous Underwater Vehicle. Chin. J. Mech. Eng. **31**(1), 110 (2018)
25. Bing, S., Wenyang, G., Man, M., Zhu, D., Yang Simon, X.: Cascaded UUV trajectory tracking control based on model predictive and sliding mode control. J. Mar. Sci. Technol. Taiw. **25**(6), 671–679 (2017)
26. Wang, M., Yanlu, Z., Dong, H.: Trajectory tracking control of a bionic robotic fish based on iterative learning. Sci. China Inf. Sci. **63**(7), 170202 (2020). https://doi.org/10.1007/s11432-019-2760-5
27. Zheng, X.W., Chen, H., Jiao, O.Y., Xiong, M.L., Zhang, W., Xie, G.M.: Model Predictive Tracking Control Design for a Robotic Fish with Controllable Barycentre. 45th Annual Conference of the IEEE Industrial Electronics Society (IECON), 5237–5242 (2019)
28. Bruggemann, S., Possieri, C.: On the use of difference of log-sum-Exp neural networks to solve data-driven model predictive control tracking problems. IEEE Control Syst. Lett. **5**(4), 1267–1272 (2021)
29. Wang, W., Dai, X., Li, L., Gheneti, B.H., Ding, Y., Yu, J.Z., Xie, G.M.: Threedimensional modeling of a fin-actuated robotic fish with multimodal swimming. IEEE/ASME Trans. Mechatron. **23**(4), 1641–1652 (2018)
30. Tian, R.Y., Li, L., Wang, W., Chang, X.H., Ravi, S., Xie, G.M.: CFD based parameter tuning for motion control of robotic fish. Bioinspir. Biomim. **15**(2), 026008 (2020). https://doi.org/10.1088/1748-3190/ab6b6c
31. Yang, Y., Wang, J., Wu, Z., Yu, J.: Fault tolerant control method for bionic robotic fish driven by CPG [J]. Engineering. **4**(6), 253–269 (2018)
32. Korkmaz, N., Öztürk, İ., Kiliç, R.: Modeling, simulation, and implementation issues of CPGs for neuromorphic engineering applications[J]. Comput. Appl. Eng. Educ. **26**(4), 782–803 (2018)
33. Zhao, J.X., Iwasaki, T.: CPG control for harmonic motion of assistive robot with human motor control identification. IEEE Trans. Control Syst. Technol. **28**(4), 1323–1336 (2020)
34. Lu, Q., Zhang, Z.C., Yue, C.: The programmable CPG model based on Matsuoka oscillator and its application to robot locomotion. Int. J. Model. Simul. Sci. Comput. **11**(3), 2050018 (2020). https://doi.org/10.1142/S179396232050018X
35. Wang, B.R., Zhang, K., Yang, X.F., Cui, X.H.: The gait planning of hexapod robot based on CPG with feedback. Int. J. Adv. Robot. Syst. **17**(3), (2020). https://doi.org/10.1177/1729881420930503
36. Shengbo, L., Wang, J., Keqiang, L.: Soft Constraint Linear Model Predictive Control System Stability Method[J]. J. Qing Univ. Nat. Sci. Ed. (11), 1848–1852 (2010)
37. Suebsaiprom, P., Lin, C.-L.: Maneuverability modeling and trajectory tracking forfish robot. Control. Eng. Pract. **45**, 22–36 (2015)
38. Shin, K.J.: Robot fish tracking control using an optical flow object-detecting algorithm. IEIE Trans. Smart Process. Comput. **5**(6), 375–382 (2016)



**Zheping Yan** received the B.E. degree in nuclear power plants in 1994, the M.E. degree in special auxiliary devices and systems for marine and marine engineering in 1997, and the Ph.D. degree in control theory and control engineering in 2001 from Harbin Engineering University. He is currently a professor at the Institute of Marine Equipment and Control Technology of Harbin Engineering University. His research interests include underwater unmanned vehicle integration and testing, marine equipment automation and intelligent technology, and underwater robot technology.

**Haoyu Yang** received the B.E. degree in mechanical engineering and automation from Shandong Jianzhu University in 2016 and the M.E. degree in mechanical engineering from Harbin Engineering University in 2019. He is currently pursuing the Ph.D. degree in Control Science and Engineering at Harbin Engineering University. His research interests include robotics and neural network control.

**Wei Zhang** received the M.E. degree and the Ph.D. degree in control theory and control engineering from Harbin Engineering University in 2004 and 2006, respectively. He is currently a professor at the Institute of Marine Equipment and Control Technology of Harbin Engineering University. His research interests include the overall design of underwater unmanned vehicle, mathematical modeling, intelligent control and data fusion.

**Qingshuo Gong** received the B.E. degree in mathematics and applied mathematics from Henan University of Science and Technology in 2019. He is currently pursuing the Ph.D. degree in Control Science and Engineering at Harbin Engineering University. His research interests include robotic control and electrical control technology.

**Fantai Lin** received the B.E. degree in measurement and control technology and instrumentation from North China Electric Power University in 2019. He is currently pursuing the M.E. degree in control science and engineering at Harbin Engineering University. His research interests include robotics and neural network control.

**Yu Zhang** graduated from Northeast Forestry University in 2018 with a bachelor's degree and is currently pursuing a doctorate degree in control science and engineering from Harbin Engineering University. His research interests include underwater robotics and sliding mode control.